Received: 5 December 2023 | Revised: 7 April 2024 | Accepted: 27 May 2024 | Published online: 6 June 2024

RESEARCH ARTICLE

Journal of Optics and Photonics Research
2024, Vol. 00(00) 1–9
DOI: 10.47852/bonviewJOPR42022235

BON VIEW PUBLISHING

Study and Analysis of Modulation Schemes for Underwater Optical Wireless Communication

Prasant Kumar Sahu[1,*] **and Debalina Ghosh**[1]

[1]*School of Electrical Sciences, Indian Institute of Technology Bhubaneswar, India*

Abstract: Communication technology is poised to play a crucial role in advancing the study of climate change, facilitating the monitoring of shifts in biological, biogeochemical, evolutionary, and ecological aspects within marine and oceanic environments. Additionally, it is imperative to ensure the efficient operation of underwater sensor networks, unmanned underwater vehicles, submarines, ships, buoys, and divers. However, existing underwater acoustic communication technology falls short of delivering the high data rates required for comprehensive investigation and surveillance in these environments and facilities. In response to this challenge, optical wireless communication has emerged as a promising alternative. This study focuses on the design and examination of an underwater optical communication link capable of communication over a horizontal distance of up to 130 meters at a depth of 40 meters. The proposed system is rigorously assessed under clear ocean conditions, considering a bit rate of 15 Gbps and employing both differential quadrature phase shift keying) technique and orthogonal frequency division multiplexing-quadrature amplitude modulation technique.

Keywords: attenuation, bit error rate, differential quadrature phase shift keying, intensity modulation and direct detection, orthogonal frequency division multiplexing-quadrature amplitude modulation, optisystem 21

1. Introduction

Underwater acoustic systems have achieved significant success due to their capacity for long-distance communication. However, the performance of these systems is constrained by inherent physical limitations that result in bandwidth restrictions, higher latency, transmission losses, multi-path propagation loss, and Doppler spread. These constraints pose challenges for the operation of sensor networks, unmanned oceanic vehicle communication, and pollution detection devices, etc. Additionally, the acoustic systems' performance is limited due to their capacity to transfer limited data rates and significantly higher latency. To solve the problems related to underwater acoustic systems, researchers are working extensively on the underwater wireless optical communication (UWOC) system.

UWOC is gaining the attention of researchers due to its ability to support higher data rates when compared to traditional acoustic communication methods. Its applications extend across military, submarine communication, underwater sensor node communication, sensor networks, unmanned oceanic vehicle communication, and pollution detection. In 1963, Duntley suggested that light within the blue and green spectrum undergoes relatively low attenuation in seawater [1]. This hypothesis was experimentally substantiated merely three years later by Gilbert et al. [2]. Researchers also explore the turbulence-induced modulation transfer functions at specific average salinity concentrations [3]. The initial findings from the Salinity processes in the upper-ocean regional study discuss understanding patterns and variability in sea surface salinity. In contrast to conventional underwater acoustic communication, UWOC offers advantages such as high bandwidth, low latency, low power consumption, and freedom from EMI/EMC as well as support for high bitrate applications [1–12].

Despite its merits, UWOC faces a significant hurdle in the form of underwater optical turbulence, which poses challenges to the effective reception of optical waves over extended underwater distances, compounded by absorption and scattering phenomena. Numerous studies investigated the impact of underwater turbulence on the propagation of optical waves and, consequently, on the received optical signals [1, 2, 5, 6, 9, 11, 13]. However, the inherent optical properties of water, including absorption and scattering, impose limitations on the transmission distances of UWOC systems, restricting them to the order of tens of meters [5, 10, 12, 14]. These constraints significantly impact the performance of UWOC links. Experimental reports on the effects of different salt concentrations in underwater optical communication are complemented by proposed mathematical models describing saline water channels [2, 3]. The channel capacity of OWC systems in the presence of intersymbol interference (ISI) salinity-induced oceanic turbulence is studied in Du et al. [14]. The establishment of long-distance, high-speed wireless optical transmission links presents a promising solution for underwater communication including data, images, and video transmissions, as demonstrated by several experimental studies achieving data rates beyond several Mbps [14–16]. Unlike free-space optical communication, research in UWOC has traditionally been confined to military applications.

*Corresponding author: Prasant Kumar Sahu, School of Electrical Sciences, Indian Institute of Technology Bhubaneswar, India. Email: pks@iitbbs.ac.in

Huang et al. [17] introduced and experimentally validated a self-interference cancellation technique for an in-band full-duplex (IBFD) UWOC system. Notably, they achieved a simultaneous data rate of 100 Mbps for both the uplink and downlink with the IBFD-based UWOC framework. Wang et al. [18] proposed and experimentally investigated the UWOC system utilizing a multi-pixel photon counter (MPPC) as the receiver and orthogonal frequency division multiplexing (OFDM). Meanwhile, Ji et al. [19] explored UWOC performance using single-photon avalanche diode and non-return-to-zero on-off keying modulation, achieving a system designed for a bitrate under 1 Mbps. Shen et al. [20] proposed a MPPC-based UWOC system with a single LED employing position modulation and a PVC pipe. The system demonstrated acceptable performance up to a depth of 46 meters, surpassing this depth resulted in bit error rates (BERs) below the forward error correction limit.

Han et al. [21] proposed a UWOC system employing a transmitter with a 150° divergence angle and more than 90% uniformity of radiation intensity using an LED array. However, the analysis focused on a bit rate of 19 Mbps over an 8-meter communication distance. Almaymoni et al. [22] successfully investigated UWOC performance by using VCSEL at ~645 nm. The considered output power was ~2 mW. The Authors achieved a data rate of 2-Gb/s by deploying direct-current biased orthogonal frequency division multiplexing. Tsai et al. [23] presented a review on high-speed visible light-based optical wireless communication. In this work, the Authors have shown the importance of the blue/violet laser diode (LDs) as a promising transmitter for underwater point-to-point transmission owing to its extremely low power extinction in water. Ali et al. [24] described the performance analysis of UWOCs using OFDM and MIMO techniques. Also, have studies on the underwater attenuation-related disturbances.

Tabeshnezhad and Pourmina [25] analyzed the outage probability of relay-assisted UWOC systems with OOK modulation and a decode-and-forward relaying scheme. However, achieving longer communication ranges remains challenging due to design complexity. Willner et al. [26] highlighted the design of an orbital angular momentum-based spatial division multiplexing system for underwater optical communication in high bitrate scenarios. Nevertheless, most high bitrate systems were observed to be range-limited ($\leq$ 10 meters). Kaushal and Kaddoum [27] reported a review article emphasizing the use of single-photon receivers.

In Akhoundi et al. [28], a cellular underwater wireless optical code-division multiple-access network based on optical orthogonal codes was implemented, featuring an experimental prototype with transmitters, receivers, and field programmable gate arrays. Chung-Yi Li et al. explored an 82-meter, 9 Gbps four-level pulse amplitude modulation free-space optical (FSO) plastic optical fiber (POF) UWOC convergent system using a 405-nm blue-light injection-locked LD in Li et al. [29]. The authors achieved signal transmission over a 50-meter FSO link and 30-meter graded-index POF transportation in a 2-meter clear ocean underwater channel.

Li et al. [30] presented a proposal for a fast numerical solution for the steady-state radiative transfer equation to calculate the optical path loss in various water types due to absorption and scattering. Khalighi et al. [31] have proposed the use of pulse amplitude modulation together with frequency-domain equalization at the receiver to boost the communication rate beyond the bandwidth limitation of the optoelectronic components. The use of autonomous underwater vehicles (AUV) utilizing optical wireless communication networks is growing day by day. However, for such networks coverage is a main issue. Palitharathna et al. [32] developed and analyzed an efficient algorithm using four-adjacency or eight-adjacency maneuvers to find the optimum AUV positions such that the number of sensors assigned to a cell is maximized. Boluda-Ruiz et al. [33] have analyzed the unified impulse response modeling of underwater optical scattering channels based on the superposition of one impulsive component, and one dispersive component with two degrees of freedom. The work also reports the impact of ISI on the data rate. The tolerance of UOWC link misalignment using turbid water is analyzed in Sun et al. [34]. Experimentally, the authors have shown the possibility of light coverage area enhancement in turbid water. Mohammadi et al. [35] presented a review work on "Full-Duplex Communication: Current Solutions, Future Trends, and Open Issues." The work mostly addresses the potential research directions, open challenges, and applications for future full-duplex-assisted wireless, including cell-free massive MIMO, mmWave communications, UAV, and RISs.

This paper's objective is to explore the measures for enhancing the performance of an underwater optical wireless communication system. The analysis of the underwater communication system employs the differential quadrature phase shift keying (DQPSK) technique and orthogonal frequency division multiplexing-quadrature amplitude modulation (OFDM-QAM) technique. While much of the existing work primarily concentrates on evaluating performance improvements in terms of bitrate enhancement using phase shift keying, differential phase shift keying (DPSK), or quadrature phase shift keying (QPSK), underwater optical wireless state-of-the-art systems predominantly employ intensity modulation (IM) schemes with direct detection (DD). Our proposed approach encompasses the examination of both bitrate and depth of operation improvements using DQPSK modulation and OFDM-QAM. Section 2 introduces the operational principles of the proposed system, along with the block diagram, implemented using Optisystem 21. The detailed experimental setup of the proposed system is illustrated in the block diagram. Section 3 presents and discusses the simulated results, while Section 4 summarizes the paper with a concise conclusion.

2. Operational Principles

DQPSK represents a type of phase modulation wherein the carrier wave's phase shift is linked to the phase shift of the preceding symbol [7]. DQPSK employs relative phase instead of absolute phase modulation, making it resistant to a fixed phase offset resulting from potential synchronization discrepancies between the transmitter and receiver. This constant offset uniformly affects all symbols and is effectively nullified through the subtraction process. In DQPSK, the receiver determines the corresponding phase change instead of decoding each received signal individually, removing the need for a reference local carrier. Moreover, DQPSK demonstrates resilience against frequency disparities between the transmitter and receiver. Even in the presence of a frequency offset causing a time-varying phase error, as long as this error changes gradually relative to the symbol rate, the differential phase remains sufficiently accurate for reliable data transfer. The DQPSK system further provides robustness against errors induced by fading in the transmission medium. The DQPSK signal is typically generated using three concatenated Mach-Zehnder (MZ) modulators. However, our approach in this study involves employing a DPSK precoder, simulating a precoder that generates two encoded signals modulating the first and second MZ modulator. The final modulator produces the DQPSK-RZ signal.

Figure 1
NLOS channel model

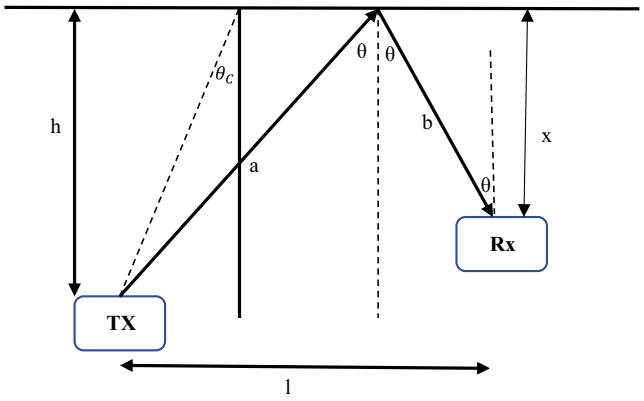

As per the available information from published literature, it is understood that attenuation is an unavoidable phenomenon arising from absorption and scattering in water for underwater optical communication. While seawater contains certain impurities, their impact on attenuation is notably lower within the visible spectrum, particularly in the blue or green zones. Therefore, the selection of the spectrum is carefully tailored to support high-speed connections. In this work, we selected the 532 nm optical source to facilitate high-speed connections. The degradation of light in seawater is contingent upon both the absorption coefficient (a (λ)) and the scattering coefficient (b (λ)). As a result, the transmission quality experiences a decline with a higher impurity rate. To quantitatively capture the attenuation phenomenon, the spectral beam attenuation coefficient (C (λ)) is introduced, and the relationship between light propagation and attenuation is mathematically expressed in Equation (1). This equation serves as a pivotal tool in understanding and optimizing underwater optical communication systems for enhanced performance in challenging aquatic environments.

$$C(\lambda) = a(\lambda) + b(\lambda) \tag{1}$$

The absorption and scattering coefficients, measured in inverse meter units, are contingent on various factors such as the contribution of water molecules, particulate algal or sediment matters, and dissolved colored organic contents. Our considered underwater optical wireless channel operates under non-line-of-sight mode (NLOS). Atypical arrangement for this is as follows:

In Figure 1, "h" is the transmitter depth and x is the receiver depth. The angle θ represents the incidence angle. θ_C is the critical angle. The distance the transmitted beam travels before hitting the surface of the water is "a." Similarly, the distance the reflected beam travels to reach the receiver is labeled as "b." The distance between the transmitter and receiver plane is labeled as "l."

The received optical power under NLOS [15] can be expressed as;

$$P_{Rx} = P_T \eta_T \eta_R \frac{A_{rec} cos(\theta)}{A_{ann}} * e^{-\frac{x+h}{\cos(\theta)} * c(\lambda)} * \frac{1}{2} \left(\left(\frac{\tan(\theta_t - \theta)}{\tan(\theta_t - \theta)} \right)^2 + \left(\frac{\sin(\theta - \theta_t)}{\sin(\theta + \theta_t)} \right)^2 \right), \quad \theta_{\min} \le \theta < \theta_C \tag{2}$$

$$P_{Rx} = P_T \eta_T \eta_R \frac{A_{rec} cos(\theta)}{A_{ann}} * e^{-\frac{x+h}{\cos(\theta)} * c(\lambda)}, \theta_C \le \theta < \theta_{max} \tag{3}$$

Figure 2
Simulated setup for underwater optical wireless communication

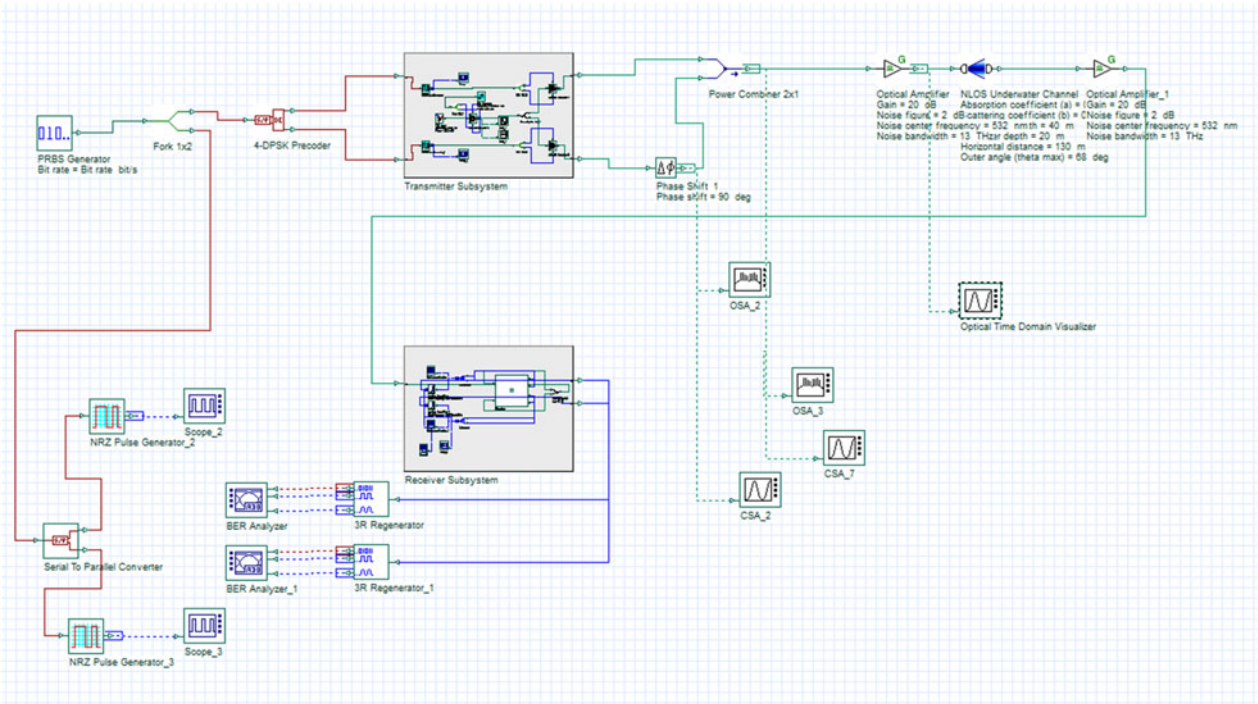

Table 1
Simulation parameters

Simulation parameters	
Bit rate	15e + 009 bps
Sample rate	60e + 009 bps
Sequence length	32768
Samples per bit	4
Guard bits	0
Symbol rate	7.5e + 009 symbols/sec
Number of samples	131072
Frequency	532 nm
Power	0.2 Watt
Linewidth	0.15 MHz
Initial phase	0
Azimuth	0
Ellipticity	0
Enabled	YES
Iterations	1
Parameterized	NO
Sample rate	60e+009 bps
Noise bandwidth	0
Noise threshold	−100 dB

Table 2
Components used for simulation

Components used in the simulation	
CW laser	X coupler_2
Pseudo-random bit sequence generator	X coupler_3
LiNbo3 Mach-Zehnder modulator 1	X coupler
LiNbo3 Mach-Zehnder modulator 2	3R regenerator
LiNbo3 Mach-Zehnder modulator 3	3R regenerator_1
Sine generator	Time delay
4-DPSK precoder	Phase shift
Photodetector PIN	Phase shift_1
Photodetector PIN_1	Low pass Bessel filter
Photodetector PIN_2	NRZ pulse generator
Photodetector PIN_3	Power splitter 1 × 2_
Time delay_1	Power combiner 2 × 1
Phase shift_2	NLOS underwater Chan
X coupler_1	Optical amplifier

Table 4
Q-Factor for DQPSK versus distance

Underwater distance between transmitter and receiver	Q-factor
130 meters	6.77
123.21 meters	7.54
89.261 meters	20.71
75.68 meters	29.71

where P_T is the average transmitter optical power, η_T is the optical efficiency of the transmitter, η_R is the optical efficiency of the receiver, θ is the incident angle between the incident TX ray and the perpendicular to the water surface, θ_t is the transmission angle of the refracted TX ray and the perpendicular to the water surface, A_{rec} is the receiver aperture area, A_{ann} is the illuminated annular area at the water surface and it is given by:

$$A_{ann} = 2\pi(x+h)^2(\cos(\theta_{max}) - cos(\theta_{min}))$$

The proposed UOWC system is depicted in Figure 2. The system's performance is evaluated through the application of IMDD, DQPSK, and OFDM-QAM techniques. As illustrated in Figure 2, the system comprises of a transmitter employing DQPSK with a 4-DPSK precoder/OFDM-QAM pulses, a wireless optical channel, an optical amplifier, and an optical receiver consisting of an avalanche photodiode as a photodetector, 3-R regenerator, low-pass Bessel filter, BER analyzer, and various visualizers for result analysis. The simulation setup components and parameters are detailed in Tables 1–3, respectively. The underwater channel considered in this scenario exhibits an attenuation of 0.043 per meter. Depending on the water type, the attenuation value can be chosen, and the communication channel distance can be adjusted to optimize the trans-reception of underwater optical signals.

3. Results and Discussion

In this proposed study, we conducted simulations for an underwater NLOS optical communication system operating at 15 Gbps. The different detrimental effects were scrutinized, with the help of Q-Factor, BER, and constellation diagrams. The Q-factor values corresponding to the increase in transmission distance for DQPSK modulation are presented in Table 4. It is evident from the table that the DQPSK system consistently surpasses the

Table 3
DQPSK parameters used for simulation

DQPSK 33% (Parallel MZM) parameters (All units are in SI units)			
Sensitivity	−100 dB	Phase (deg)	−90
Extinction ratio	30 dB	Surface incident angle (deg)	33.690068
Low pass Bessel filter parameters		Critical angle (deg)	48.461484
Cut-off frequency (Hz)	3.75E+08	Index of refraction Water	1.336388
Depth	100	Receiver area (m^2)	0.125664
Order	4	Path length (m) (variable)	72.111026
Enabled	YES	Attenuation (1/m)	0.043
Additional loss	0	Divergence loss (dB)	51.312762
		Propagation loss (dB)	13.466491
		Reflection loss (dB)	15.061369

Figure 3
Underwater IMDD system for 130 meters

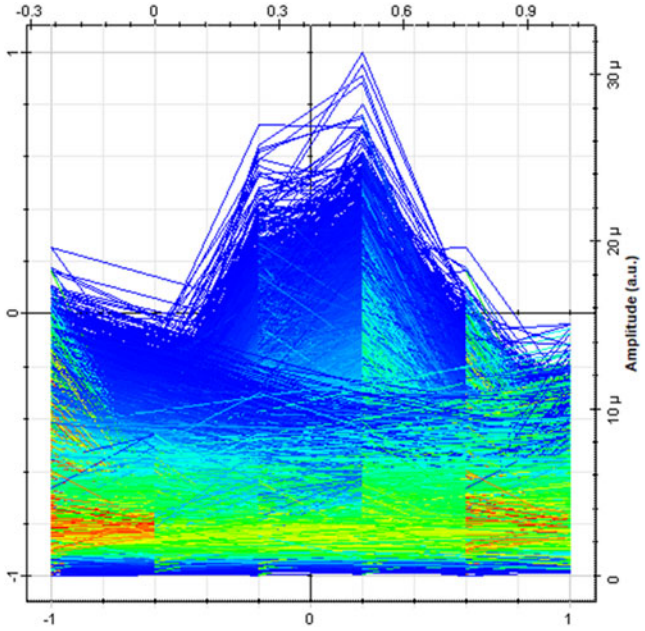

Figure 4
Response of underwater DQPSK system for a horizontal range of 130 meters

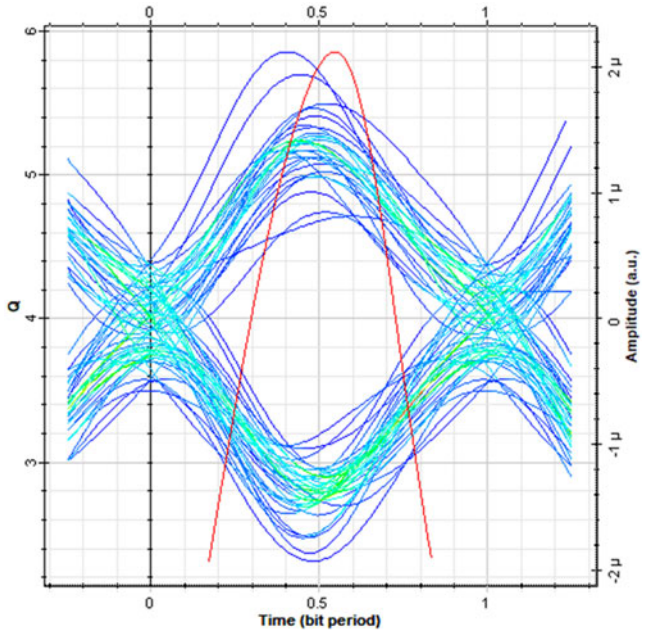

Figure 5
Response of underwater DQPSK system for a horizontal range of 123.1 meters

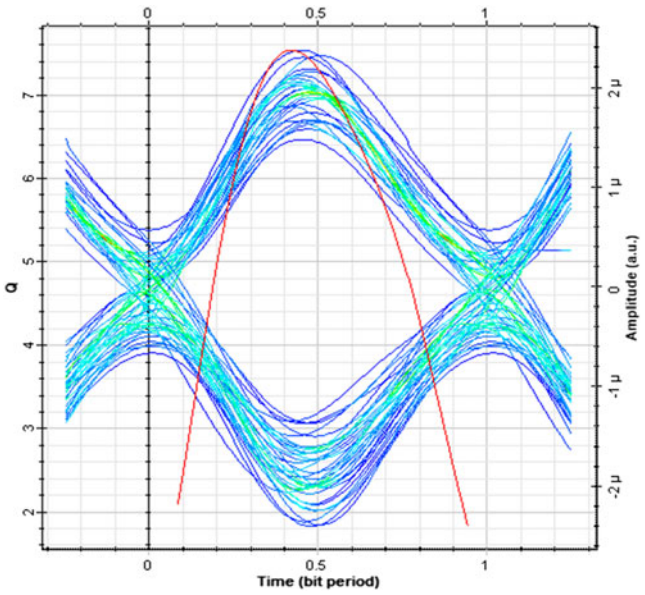

Figure 6
Response of underwater DQPSK system for a horizontal range of 89.263 meters

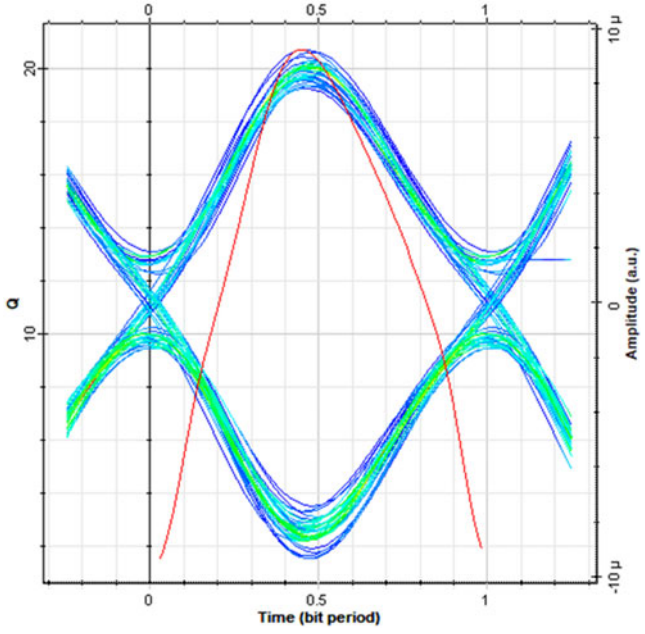

threshold value of 6.2 for all distances up to 130 meters between the transmitters and the receiver. We have first analyzed the possibility of using the IMDD system for underwater applications for a bit rate of 15 Gbps for a distance of up to 130 meters. The simulated results as shown in Figure 3 exhibit almost a closed eye due to the very high amount of non-linear effect, ISI, and jitter effect. The eye diagram, corresponding to the horizontal distance between the transmitter and receiver, is illustrated for four different scenarios (130 meters, 123.21 meters, 89.261 meters, and 75.68 meters) in Figures 4–7, respectively. The analysis provides insights into the system's performance across varying distances through examination of Q-Factor, BER, and constellation diagrams. The system's performance can be measured in terms of an eye diagram and constellation diagram. The eye diagram is useful in measuring the BER and Q-Factor. As can be seen, if the eye is open then it indicates that the transmission is error-free.

The eye diagrams are presented with noise and random jitter, which strongly depends upon the distance between the transmitter

Figure 7
Response of underwater DQPSK system for a horizontal range of 75.68 meters

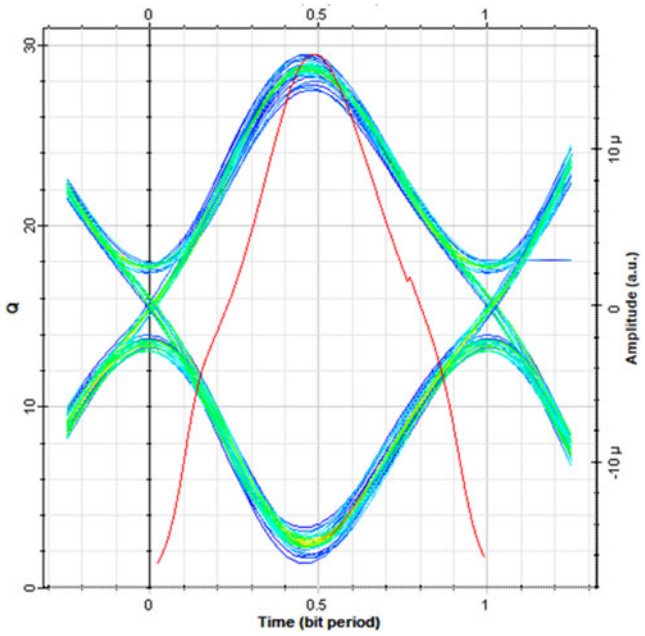

and receiver, the launch power, the non-linearity effects, the water types, etc. The vertical eye closure is mainly due to the ISI, and the horizontal eye closure is caused by deterministic jitter. The eye margins (including both the vertical and horizontal) as observed in Figures 4–7 describe the possibility of selection of decision circuit for recovering the data at the desired reference BER level.

Figure 8
Response of underwater OFDM-QAM system for a horizontal range of 130 meters

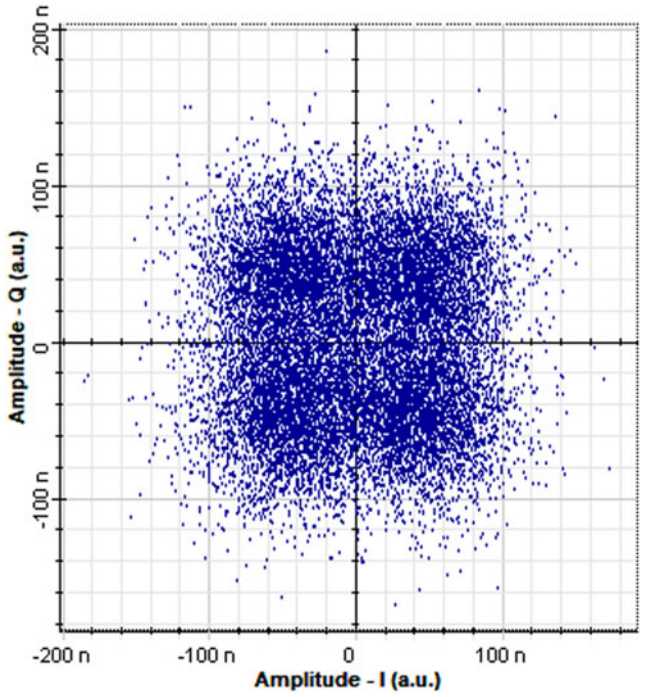

Figure 9
Response of underwater OFDM-QAM system for a horizontal range of 123.1 meters

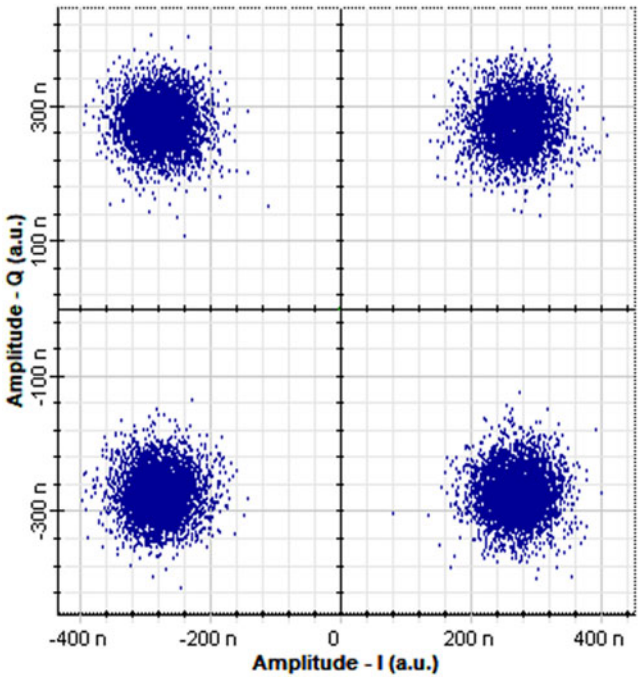

The results as presented in Figures 8–10 explain the constellation diagram of the simulated underwater OFDM-QAM system for the same four different scenarios (130 meters, 123.21 meters, 89.261 meters and 75.68 meters) for the DQPSK system. As we know, the constellation diagram demonstrates the in-phase and quadrature phase on the X and Y axes, respectively.

The effectiveness of a digital communication system is determined by how precisely the binary digits received at the detector's output align with the input signal from the transmitter side. Low SNR at the receiver side causes the constellation points to spread out randomly around their ideal positions. From Figures 8–11, it is visible that due to the low SNR at the receiver side, the points are spreading out about their ideal position. The system performance is unacceptable at 130 meters. However, for other distances as shown the system performance is comparable to the DQPSK system.

Table 5 reports the Q-factor for the considered modulation scheme for analyzing the underwater optical wireless communication system. The Q-factor is calculated by using the following expression.

$$Q = \frac{\mu_1 - \mu_0}{\sigma_1 + \sigma_0} \tag{4}$$

where μ_1 and μ_0 are average values and σ_1 and σ_0 are standard deviations of the sampled values, respectively. The results depict the advantages of selecting the DQPSK system for designing the underwater optical wireless communication system for potential applications like sensor networks, unmanned underwater vehicles, submarines, ships, and buoys, and for assisting divers.

Figure 10
Response of underwater OFDM-QAM system for a horizontal range of 89.263 meters

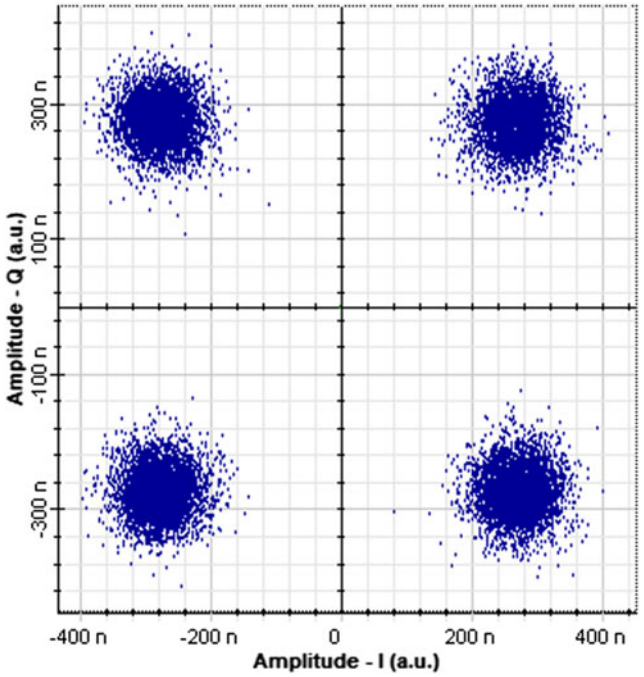

Figure 11
Response of underwater OFDM-QAM system for a horizontal range of 75.68 meters

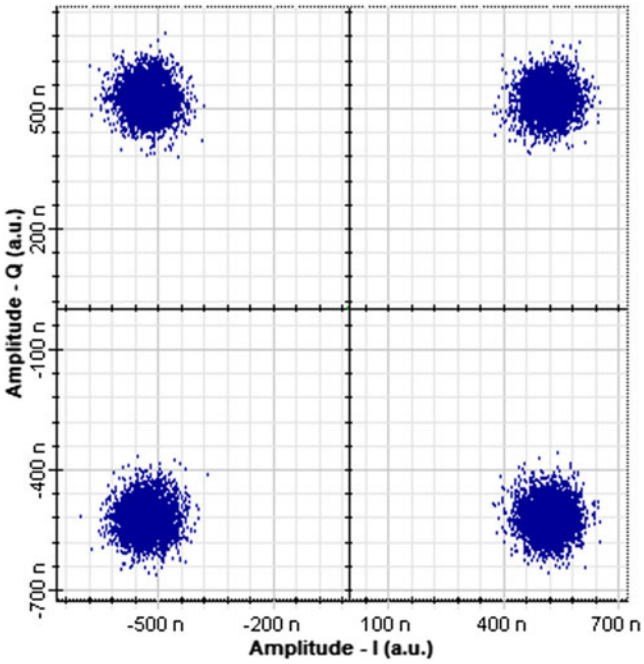

Table 5
Q-factor comparison

	Q-factors		
Distance (meters)	IMDD	DQPSK	OFDM-QAM
1	0	7.1	2.644
7.8	0	9.39	2.49
14.6	0	8.35	2.26
21.4	0	10.07	2.16
28.2	0	14.42	2.11
34.9	0	18.52	2.01
41.7	0	29.79	1.89
48.5	0	29.7	2.32
55.3	0	24.38	2.83
62.1	0	18.99	4.99
68.9	8.5	23.53	15.99
75.7	7.32	18.51	13.11
82.5	6.28	14.23	10.75
89.3	5.3	13.88	8.4
96.0	4.51	14.36	6.16
102.8	3.76	9.03	4.89
109.6	0	10.077	3.51
116.4	0	7.85	2.64
123.2	0	8.19	1.82
130	0	6.08	1.71

4. Conclusion

In summary, this study comprehensively analyzes the performance parameters of an underwater optical wireless communication system employing IMDD, DQPSK, and OFDM-QAM modulation schemes. The results reveal that distortion tends to increase with distance. Conclusively, the DQPSK modulation scheme emerged as the most effective, displaying superior performance in terms of eye-opening, Q-Factor, and maximum link reach. It serves as a promising platform for extending the communication range in underwater optical communication, demonstrating robustness against errors induced by phase shifts, and fading in the transmission medium. However, it is worth noting that DQPSK is relatively more complex to implement compared to other modulation schemes such as binary phase shift keying (BPSK) and QPSK. We also conclude that the spectrally efficient modulation technique of OFDM-QAM is suitable for underwater optical communication for underwater ranges up to 123 meters for some specific distances because of its ability to mitigate power penalties resulting from polarization mode dispersion.

Ethical Statement

This study does not contain any studies with human or animal subjects performed by any of the authors.

Conflicts of Interest

The authors declare that they have no conflicts of interest to this work.

Data Availability Statement

Data available on request from the corresponding author upon reasonable request.

References

[1] Duntley, S. Q. (1963). Light in the sea. *Journal of the Optical Society of America*, *53*(2), 214–233. https://doi.org/10.1364/JOSA.53.000214

[2] Gilbert, G. D., Stoner, T. R., & Jernigan, J. L. (1966). Underwater experiments on the polarization, coherence, and scattering properties of a pulsed blue-green laser. In *Proceedings of Underwater Photo-Optical Instrumentation Applications*, 8–14. https://doi.org/10.1117/12.971001

[3] Lindstrom, E., Bryan, F., & Schmitt, R. (2015). SPURS: Salinity processes in the upper-ocean regional study. *Oceanography*, *28*(1), 14–19.

[4] Tang, S., Dong, Y., & Zhang, X. (2012). On link misalignment for underwater wireless optical communications. *IEEE Communications Letters*, *16*(10), 1688–1690. https://doi.org/10.1109/LCOMM.2012.081612.121225

[5] Lu, H. H., Li, C. Y., Lin, H. H., Tsai, W. S., Chu, C. A., Chen, B. R., & Wu, C. J. (2016). An 8 m/9.6 Gbps underwater wireless optical communication system. *IEEE Photonics Journal*, *8*(5), 7906107. https://doi.org/10.1109/JPHOT.2016.2601778

[6] Boucouvalas, A. C., Peppas, K. P., Yiannopoulos, K., & Ghassemlooy, Z. (2016). Underwater optical wireless communications with optical amplification and spatial diversity. *IEEE Photonics Technology Letters*, *28*(22), 2613–2616. https://doi.org/10.1109/LPT.2016.2607278

[7] Roy, A., Nemade, H. B., Bhattacharjee, R., & Kushwah, V. (2017). DQPSK modulation and demodulation using SAW device. *IET Communications*, *11*(17), 2630–2636. https://doi.org/10.1049/iet-com.2017.0821

[8] Diamant, R., Campagnaro, F., de Filippo de Grazia, M., Casari, P., Testolin, A., Sanjuan Calzado, V., & Zorzi, M. (2017). On the relationship between the underwater acoustic and optical channels. *IEEE Transactions on Wireless Communications*, *16*(12), 8037–8051. https://doi.org/10.1109/TWC.2017.2756055

[9] Jamali, M. V., Nabavi, P., & Salehi, J. A. (2018). MIMO underwater visible light communications: Comprehensive channel study, performance analysis, and multiple-symbol detection. *IEEE Transactions on Vehicular Technology*, *67*(9), 8223–8237. https://doi.org/10.1109/TVT.2018.2840505

[10] Guo, Y., Wang, X., & Fu, M. (2020). QAM–OFDM transmission in underwater wireless optical communication system with limited resolution DAC. *Optical and Quantum Electronics*, *52*(9), 419. https://doi.org/10.1007/s11082-020-02529-9

[11] Kumar, L. B., Naik, R. P., Krishnan, P., Raj, A. A. B., Majumdar, A. K., & Chung, W. Y. (2022). RIS assisted triple-hop RF-FSO convergent with UWOC system. *IEEE Access*, *10*, 66564–66575. https://doi.org/10.1109/ACCESS.2022.3185123

[12] Vijayakumari, P., Chanthirasekaran, K., Jayamani, K., Nirmala, P., & ThandaiahPrabu, R. (2022). BIT error rate analysis of various water samples in underwater wireless optical communication system. In *International Conference on Advances in Computing, Communication and Applied Informatics*, 1–5. https://doi.org/10.1109/ACCAI53970.2022.9752642

[13] Ata, Y., & Kiasaleh, K. (2023). Analysis of optical wireless communication links in turbulent underwater channels with wide range of water parameters. *IEEE Transactions on Vehicular Technology*, *72*(5), 6363–6374. https://doi.org/10.1109/TVT.2023.3235823

[14] Du, Z., Ge, W., Cai, C., Wang, H., Song, G., Xiong, J., . . . , & Xu, J. (2023). 90-m/660-Mbps underwater wireless optical communication enabled by interleaved single-carrier FDM scheme combined with sparse weight-initiated DNN equalizer. *Journal of Lightwave Technology*, *41*(16), 5310–5320. https://doi.org/10.1109/JLT.2023.3262352

[15] Arnon, S., & Kedar, D. (2009). Non-line-of-sight underwater optical wireless communication network. *Journal of the Optical Society of America A*, *26*(3), 530–539. https://doi.org/10.1364/JOSAA.26.000530

[16] Luo, H., Wang, X., Bu, F., Yang, Y., Ruby, R., & Wu, K. (2023). Underwater real-time video transmission via wireless optical channels with swarms of AUVs. *IEEE Transactions on Vehicular Technology*, *72*(11), 14688–14703. https://doi.org/10.1109/TVT.2023.3280121

[17] Huang, L., Zhang, L., Jiang, R., Chen, Z., Chen, Z., & Li, Z. (2024). Reference signal aided self-interference cancellation for in band full duplex underwater wireless optical communication. *Optics Communications*, *554*, 130159. https://doi.org/10.1016/j.optcom.2023.130159

[18] Wang, J., Yang, X., Lv, W., Yu, C., Wu, J., Zhao, M., . . . , & Xu, J. (2019). Underwater wireless optical communication based on multi-pixel photon counter and OFDM modulation. *Optics Communications*, *451*, 181–185. https://doi.org/10.1016/j.optcom.2019.06.053

[19] Ji, Y., Wu, G., & Zuo, Y. (2018). Performance analysis of SPAD-based underwater wireless optical communication systems. *Procedia Computer Science*, *131*, 1134–1141. https://doi.org/10.1016/j.procs.2018.04.282

[20] Shen, J., Wang, J., Yu, C., Chen, X., Wu, J., Zhao, M., . . . , & Xu, J. (2019). Single LED-based 46-m underwater wireless optical communication enabled by a multi-pixel photon counter with digital output. *Optics Communications*, *438*, 78–82. https://doi.org/10.1016/j.optcom.2019.01.031

[21] Han, B., Zhao, W., Zheng, Y., Meng, J., Wang, T., Han, Y., . . . , & Xie, X. (2019). Experimental demonstration of quasi-omni-directional transmitter for underwater wireless optical communication based on blue LED array and freeform lens. *Optics Communications*, *434*, 184–190. https://doi.org/10.1016/j.optcom.2018.10.037

[22] Almaymoni, N., Alkhazragi, O., Gunawan, W. H., Melinte, G., Ng, T. K., & Ooi, B. S. (2024). High-speed 645-nm VCSELs for low-scattering-loss Gb/s underwater wireless optical communications. *IEEE Photonics Technology Letters*, *36*(6), 377–380. https://doi.org/10.1109/LPT.2024.3360229

[23] Tsai, C. T., Cheng, C. H., Kuo, H. C., & Lin, G. R. (2019). Toward high-speed visible laser lighting based optical wireless communications. *Progress in Quantum Electronics*, *67*, 100225. https://doi.org/10.1016/j.pquantelec.2019.100225

[24] Ali, A. H., Kadhim, S. A., & Azzawi, H. M. (2018). Next generation UWOC system based on MIMO and QAM-OFDM modulation techniques. In *Third Scientific Conference of Electrical Engineering*, 235–240. https://doi.org/10.1109/SCEE.2018.8684207

[25] Tabeshnezhad, A., & Pourmina, M. A. (2017). Outage analysis of relay-assisted underwater wireless optical communication systems. *Optics Communications*, *405*, 297–305. https://doi.org/10.1016/j.optcom.2017.08.051.

[26] Willner, A. E., Zhao, Z., Ren, Y., Li, L., Xie, G., Song, H., . . . , & Pang, K. (2018). Underwater optical communications using orbital angular momentum-based spatial division multiplexing. *Optics Communications*, *408*, 21–25. https://doi.org/10.1016/j.optcom.2017.08.002

[27] Kaushal, H., & Kaddoum, G. (2016). Underwater optical wireless communication. *IEEE Access*, *4*, 1518–1547. https://doi.org/10.1109/ACCESS.2016.2552538

[28] Akhoundi, F., Salehi, J. A., & Tashakori, A. (2015). Cellular underwater wireless optical CDMA network: Performance analysis and implementation concepts. *IEEE Transactions on Communications*, *63*(3), 882–891. https://doi.org/10.1109/TCOMM.2015.2400441

[29] Li, C. Y., Lu, H. H., Wang, Y. C., Wang, Z. H., Su, C. W., Lu, Y. F., & Tsai, W. S. (2019). An 82-m 9 Gb/s PAM4 FSO-POF-UWOC convergent system. *IEEE Photonics Journal*, *11*(1), 1–9. https://doi.org/10.1109/JPHOT.2018.2890514

[30] Li, C., Park, K. H., & Alouini, M. S. (2015). On the use of a direct radiative transfer equation solver for path loss calculation in underwater optical wireless channels. *IEEE Wireless Communications Letters*, *4*(5), 561–564. https://doi.org/10.1109/LWC.2015.2459697

[31] Khalighi, M. A., Akhouayri, H., & Hranilovic, S. (2020). Silicon-photomultiplier-based underwater wireless optical communication using pulse-amplitude modulation. *IEEE Journal of Oceanic Engineering*, *45*(4), 1611–1621. https://doi.org/10.1109/JOE.2019.2923501

[32] Palitharathna, K. W. S., Suraweera, H. A., Godaliyadda, R. I., Herath, V. R., & Thompson, J. S. (2020). Multi-AUV placement for coverage maximization in underwater optical wireless sensor networks. In *Global Oceans, 2020*, 1–8. https://doi.org/10.1109/IEEECONF38699.2020.9389126

[33] Boluda-Ruiz, R., Rico-Pinazo, P., Castillo-Vázquez, B., García-Zambrana, A., & Qaraqe, K. (2020). Impulse response modeling of underwater optical scattering channels for wireless communication. *IEEE Photonics Journal*, *12*(4), 1–14. https://doi.org/10.1109/JPHOT.2020.3012302

[34] Sun, Q., Huang, N., Liu, W., & Xu, Z. (2023). A robust receiver comprising turbid water for LD-based UOWC System. In *IEEE 11th International Conference on Information, Communication and Networks*, 167–171. https://doi.org/10.1109/ICICN59530.2023.10392989

[35] Mohammadi, M., Mobini, Z., Galappaththige, D., & Tellambura, C. (2023). A comprehensive survey on full-duplex communication: Current solutions, future trends, and open issues. *IEEE Communications Surveys & Tutorials*, *25*(4), 2190–2244. https://doi.org/10.1109/COMST.2023.3318198

How to Cite: Sahu, P. K., & Ghosh, D. (2024). Study and Analysis of Modulation Schemes for Underwater Optical Wireless Communication. *Journal of Optics and Photonics Research*. https://doi.org/10.47852/bonviewJOPR42022235